Structure of the γ-chain of the human IgE $Fc_εR1$ receptor: NMR and molecular dynamics studies

Megan K. Eisenbraun,[a] Geoffrey E. Hawkes *[a] and Brian G. Carter †[b]

[a] *Structural Chemistry Group, Department of Chemistry, Queen Mary & Westfield College, Mile End Road, London, UK E1 4NS*
[b] *Glaxo Group Research, Greenford Road, Greenford, Middlesex, UK UB6 0HE*

Received (in Cambridge, UK) 16th November 1999, Accepted 11th May 2000
Published on the Web 15th June 2000

The solution structure of the 37-residue intracellular γ-chain of the human $Fc_εR1$ receptor protein has been determined using high field ^1H nuclear magnetic resonance (NMR) spectroscopy combined with molecular dynamics simulations. Two closely related groups of α-helical structures were found, with disruptions of the helix between residues 20 to 24; for one group the disruption is a type I β-turn, and in the second this region is less structured and acts as a loose 'hinge' between the α-helical regions. All structures exhibited a major and a minor hydrophobic region. The two tyrosines of the ARAM (antigen recognition activation motif) consensus motif lie on a single face of the helix, as do the two hydrophobic ARAM leucine and isoleucine residues. Three of the five threonines define a third face. These data are used to propose a model for the *in vivo* dimer of the γ-chain which is consistent with the susceptibility of the tyrosines and threonines to phosphorylation as an important feature of signal transduction.

Introduction

When an allergen enters the body it results in the production of allergen specific immunoglobulin E (IgE) which binds *via* its Fc region to the high affinity IgE receptor ($Fc_εR1$) located on the surface of mast cells. This binding sensitises the cell to subsequent encounters with the allergen. During such encounters the activation of the $Fc_εR1$ receptor triggers a cascade of intracellular events that culminates in the release of mediators (*e.g.* histamine) responsible for the hypersensitivity reaction.[1] The cascade of intracellular events leading to the release of the mediators is a matter of considerable current interest.

The $Fc_εR1$ receptor consists of four transmembrane polypeptides, an α, a β and two γ chains. The two γ chains are identical and are disulfide linked by two cysteine residues on the cytoplasmic side of the transmembrane segment, and the amino acid sequence of the γ-chain is: ARLKIQVRKAAIT SYEKSDGVYTGLSTRNQETYETIK. The γ-chain of the $Fc_εR1$ receptor has been shown to be the same as the FcγRIII γ-chain[2] and shows 55% amino acid identity with the T-cell antigen receptor (TCR) ζ chain.[3,4] Reth[5] discovered a sequence motif common in the cytoplasmic tails of several antigen receptors of T- and B-cells as well as the $Fc_εR1$ receptor β- and γ-chains. This conserved sequence is based on tyrosine, leucine (or isoleucine) and aspartic acid residues and is often referred to as the ARAM (antigen recognition activation motif), comprising Asp-19, Tyr-22, Leu-25, Tyr-33 and Ile-36. As all these cytoplasmic tails are involved in signal transduction it may be assumed that the mechanisms involving these motifs are similar. It has been shown that activation of these transmembrane receptors results in phosphorylation of tyrosine residues in the cytoplasmic tails of the receptor.[6] The further transmission of the signal is thought to depend on the recognition of the phosphorylated tyrosine region by distinctive domains, known as SH2 domains.[7] With the overall goal of elucidation of the molecular basis for the mechanism of signal transduction a first step is to determine the structure of the cytoplasmic region of the γ-chain before the phosphorylation step. This has been achieved through the combined use of high resolution ^1H nuclear magnetic resonance (NMR) spectroscopy and molecular dynamics (MD) simulations.

Results and discussion

^1H NMR analysis

Assignment of the ^1H chemical shifts was achieved using a combination of the 2-dimensional NMR experiments, COSY, NOESY and TOCSY[8] (see Fig. 1 and Fig. 2). The spin systems of the individual amino acid residues of the peptide in TFE-d_3–H_2O (65 : 35 v/v) were identified using TOCSY and COSY spectra at two temperatures, 290 and 300 K. Some spectra were measured in TFE-d_3–D_2O (65 : 35 v/v) in order to assist the identification of crosspeaks close to the water peak. Sequence specific assignments were made by the observation of inter-residue nuclear Overhauser effects (nOe's) in the NOESY spectra. In particular the N***H***–N***H***(i, i + 1) and $\boldsymbol{H_\beta}$–N***H***(i, i + 1) crosspeaks being the most useful. The final ^1H resonance assignments are given in Table 1. Wishart *et al.*[9] have shown that chemical shifts can be a useful indication of secondary structure. Excluding the first three residues, the majority of chemical shifts for the $Fc_εR1$ γ-chain in Table 1 are typical of helices, with the $H_α$, $H_β$ and $H_γ$ chemical shifts showing particularly good agreement with average helical values.[9]

Of the 37 residues in the peptide, 23 have β-methylene groups, and 11 of these gave rise to two resolved signals of which 5 pairs were stereochemically assignable as pro-*R* or pro-*S* on the basis of the intraresidue $\boldsymbol{H_\beta}$–N***H*** and $\boldsymbol{H_\alpha}$–$\boldsymbol{H_\beta}$ NOESY crosspeaks, as described by Baus.[10] The two α-protons of the glycine residues could only be distinguished after the creation of a set of initial structures using the unambiguous nOe constraints (see below).

The φ torsion angles were estimated from the $^3J_{\alpha N}$ interproton coupling constants which were measured from DQF-COSY spectra in the manner described by Neuhaus *et al.*[11] The residues for which coupling constants could be measured

† Present address: 10 Dellcott Close, Welwyn Garden City, Hertfordshire, UK AL8 7BD.

DOI: 10.1039/a909072j

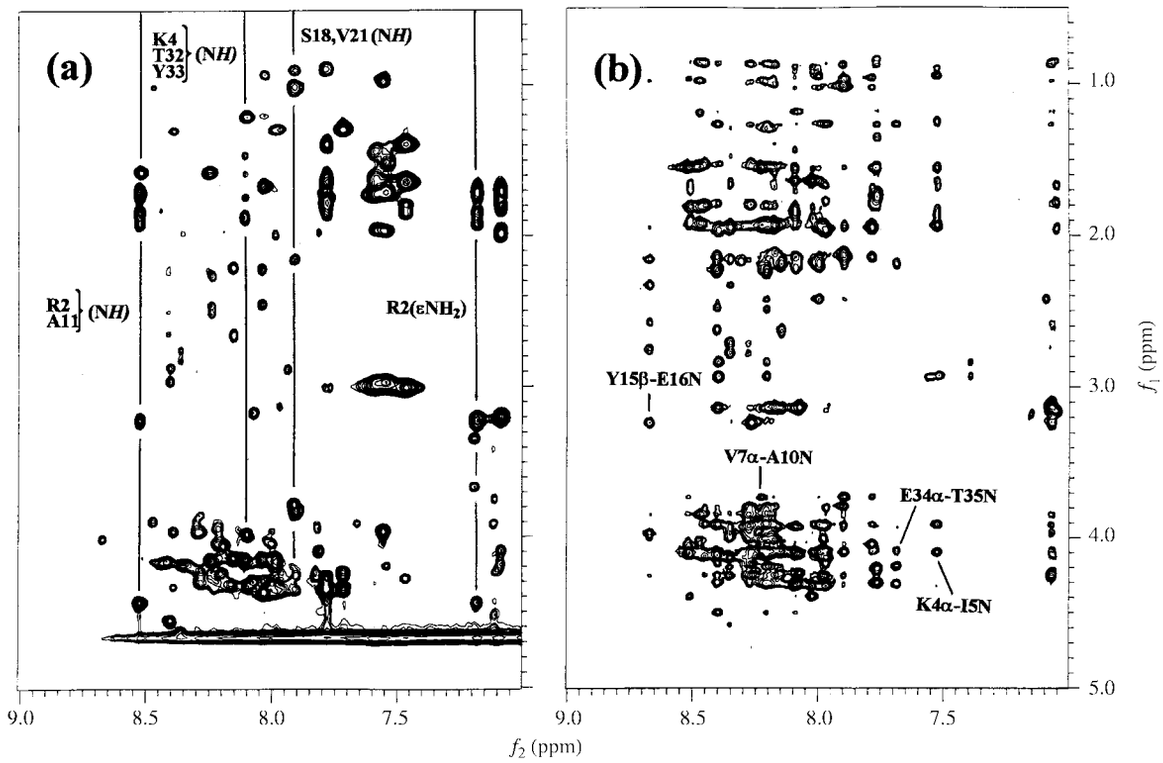

Fig. 1 Fingerprint region of the 600 MHz ^{1}H NMR spectra of the Fc$_\varepsilon$R1 γ-chain in TFE-d$_3$–water at 300 K. (a) TOCSY spectrum, the vertical lines indicate selected chemical shifts in the N*H* region. (b) NOESY spectrum with 200 ms mixing time, showing the assignment of selected inter-residue crosspeaks. Experimental conditions are given in the text.

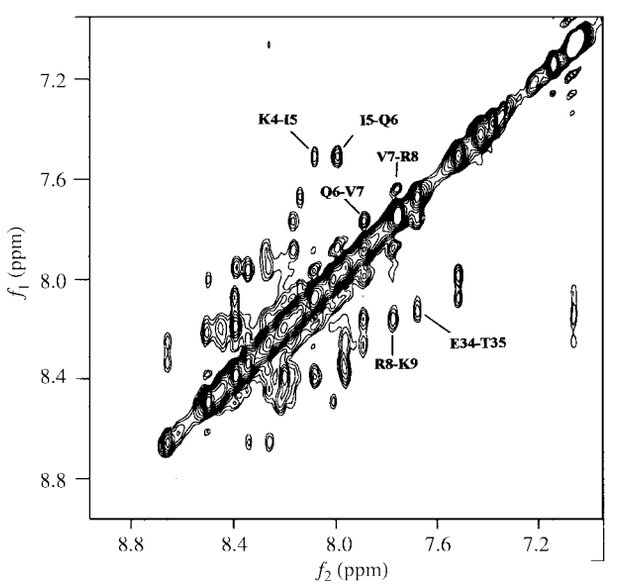

Fig. 2 High frequency region of the 600 MHz ^{1}H NOESY NMR spectrum of the Fc$_\varepsilon$R1 γ-chain in TFE-d$_3$–water at 300 K, measured with a mixing time 200 ms; selected N***H***–N***H***(*i*, *i* + 1) correlation peaks are assigned.

(all except Ala-1, Ala-10, Gly-20 and Gly-24) gave values of 5.5 Hz or less, typical of a helical structure.[12]

Estimation of distance constraints

Estimates of interproton distances can be made from crosspeak volumes in the NOESY spectra. Cross relaxation rates between pairs of protons are estimated from the variation of peak volume with the so-called 'mixing time' in the NOESY experimental pulse sequence. The cross relaxation rates are then related to internuclear separation by comparison with a 'standard' separation—usually the separation between a methylene proton pair or a pair of *ortho* protons on an aromatic ring. However errors in the final distances are likely to be large, and in order to exercise caution it was decided to use the weak, medium, strong (W,M,S) strategy[8] using the amplitude at the peak maximum measured directly from the NOESY spectrum with mixing time 200 ms. Although only strictly accurate for peaks with the same line shape, this method has been used successfully in the determination of many structures.[13,14] van der Waals radii were used as the lower bounds for the nOe constraints. The upper bounds were set to 2.5 Å (strong), 3.5 Å (medium), 5 Å (weak) and 7 Å (very weak). The results were compared with the appearance of peaks in the NOESY spectra measured using mixing times of 50 ms and 100 ms to confirm the accuracy of the peaks' intensity classifications. Crosspeaks from the 200 ms, 300 K, NOESY spectrum were grouped into three categories: (a) *Unambiguously assigned*—the chemical shifts of both protons are clearly resolved; (b) *Ambiguously assigned*—the chemical shifts of one or both of the protons are not clearly resolved, but the most probable connection can easily be made; (c) *Unassigned*—crosspeaks involving two or more probable connections between proton pairs, or long range connections that appear unsupported by additional nOe data.

Centroid dummy atoms were used for unresolved methylene proton pairs and for methyl groups, and appropriate distance corrections were made as described by Wüthrich *et al.*[15] Because of fast intramolecular motion of the methyl groups, the distances derived may be too short[16] and therefore the upper distance boundaries for nOe's involving methyl groups were increased to 7 Å for weak nOe's, 5 Å for medium nOe's and 3.5 Å for strong nOe's. In this way more than 170 interproton distances were obtained. In order to be able to use nOe's from ambiguous assignments the following procedure was followed. As described below the variable target function program DIANA[16] was used to create 50 initial structures using the unambiguous distances and the 33 φ torsion angles from the measured $^3J_{\alpha N}$ couplings. After energy minimisation these structures were used to resolve as many as possible of the ambiguous and unassigned crosspeaks. Thus an additional 33 interproton

Table 1 ^{1}H chemical shifts[a] (ppm) of the $Fc_\varepsilon R1$ γ-chain in 65% TFE-d_3 at 300 K

Residue	NH	H_α	H_β	Other ^{1}H shifts
Ala-1		4.32	1.55	
Arg-2	8.51	4.39	1.80, 1.88	1.64(γ), 3.15(δ), 7.15(ε)
Leu-3	8.02	4.32	1.62	1.62(γ), 0.96, 0.88(δ)
Lys-4	8.09	4.10	1.84	1.43(γ), 1.64(δ), 2.97(ε), 7.55(NH_2)
Ile-5	7.52	3.91	1.93	1.25, 0.95(γ), 0.90(δ)
Gln-6	8.00	4.09	2.18	2.42(γ), 6.55, 7.09(ε)
Val-7	7.89	3.72	2.13	1.02, 0.96(γ)
Arg-8	7.78	4.04	1.95, 1.79	1.67(γ), 3.16(δ), 7.05(ε)
Lys-9	8.18	4.02	1.93	1.39(γ), 1.68(δ), 2.93(ε), 7.55(NH_2)
Ala-10	8.23	4.08	1.55	
Ala-11	8.51	4.10	1.55	
Ile-12	8.47	3.84	1.91	1.19, 0.97(γ), 0.84(δ)
Thr-13	8.20	4.00	4.30	1.29(γ)
Ser-14	8.18	4.19	3.98, 4.09	
Tyr-15	8.26	4.25	3.23	7.07(C2,6), 6.76(C3,5)
Glu-16	8.66	3.96	2.16, 2.30	2.57, 2.74(γ)
Lys-17	8.35	4.13	1.94	1.48(γ), 1.67(δ)
Ser-18	7.97	4.25	3.91, 4.00	
Asp-19	8.35	4.58	2.70, 2.77	
Gly-20	8.27	3.85, 3.90		
Val-21	7.90	3.78	2.10	0.87, 1.01(γ)
Tyr-22	8.17	4.25	3.13	7.07(C2,6), 6.78(C3,5)
Thr-23	8.40	3.92	4.30	1.26(γ)
Gly-24	8.20	3.80, 3.83		
Leu-25	8.45	4.12	1.80	1.53(γ), 0.86(δ)
Ser-26	8.27	4.17	3.80, 3.91	
Thr-27	7.97	4.08	4.32	1.26(γ)
Arg-28	7.97	4.13	1.77, 1.96	1.67(γ), 3.20(δ), 7.05(ε)
Asn-29	8.40	4.50	2.83, 2.92	6.40, 7.37(NH_2)
Gln-30	8.20	4.10	2.23	2.42, 2.48(γ), 6.45, 7.03(ε)
Glu-31	8.40	4.11	2.14, 2.22	2.47, 2.61(γ)
Thr-32	8.09	3.92	4.30	1.18(γ)
Tyr-33	8.07	4.24	3.13	7.07(C2,6), 6.78(C3,5)
Glu-34	8.15	4.08	2.18	2.63(γ)
Thr-35	7.68	4.18	4.31	1.26(γ)
Ile-36	7.76	4.30	1.76	1.56(γ), 0.83, 0.87(δ)
Lys-37	7.77	4.20	1.75, 1.80	1.35(γ), 1.61(δ), 2.97(ε), 7.44(NH_2)

[a] Chemical shifts are given relative to TFE-d_3 at 3.9 ppm from TMS. The residues of the conserved Reth ARAM motif are highlighted.

distances were assigned making a total of 203 distances. The overall breakdown of the nOe derived distances was 66 intra-residue, 78 sequential inter-residue, and 59 non-sequential inter-residue distances, and the most important of these are summarised in Fig. 3.

Molecular dynamics simulations

The program DIANA was used to create 50 structures prior to MD simulated annealing by applying the parameters described by Güntert *et al.*[16] In addition to the nOe constraints, torsion angle (φ) ranges were included; these consisted of the ideal α-helix value (−57°) allowed to vary by ±20°. The torsion angle constraints on the DIANA structures were then removed before entering the simulated annealing protocol, as exact torsion angles were not obtained from the NMR data. Each of the structures was then subjected to 100 steps of conjugate gradient energy minimisation.

Electrostatic charges were calculated using the Hückel[17] and Gasteiger–Marsili[18] methods for π and σ charges respectively. Simulations of peptide structures *in vacuo* can lead to an over-abundance of intramolecular hydrogen bonds, which may cause distortions in the final structures.[19] One method of accounting for the presence of solvent is by including the relative permittivity of the solvent within the force field.[19] However, the relative permittivity for the solvent mixture was not available. Several tests on the final structure of the $Fc_\varepsilon R1$ γ-chain were performed varying the relative permittivity between 30 and 100. The effect of variation of this parameter appeared to be negligible, therefore it was decided that using the relative permittivity of water (78.30)[20] was preferable to proceeding with simulations *in vacuo*.

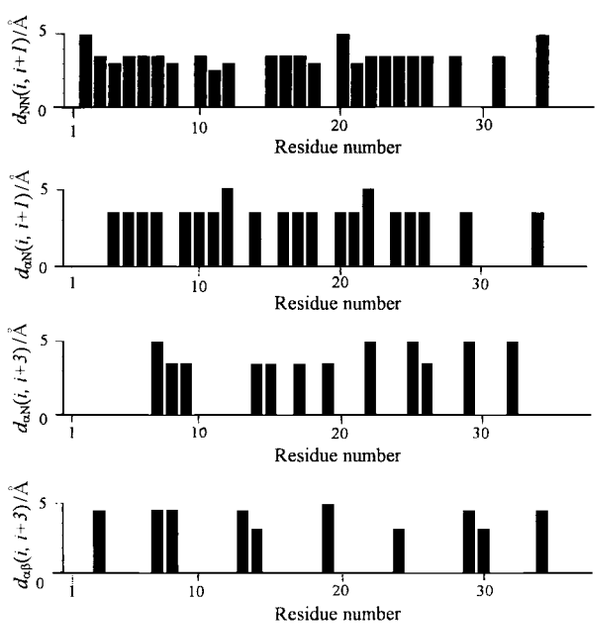

Fig. 3 The most important interproton distance constraints obtained from the analysis of the NOESY spectra. The vertical bars indicate the internuclear distance (d/Å) obtained as described in the text, and i is the amino acid residue number.

The structures were then entered into a simulated annealing routine,[21] allowing potential energy barriers to be crossed. A potential energy cut-off was used to reject structures trapped in extremely high energy conformations during the simulated

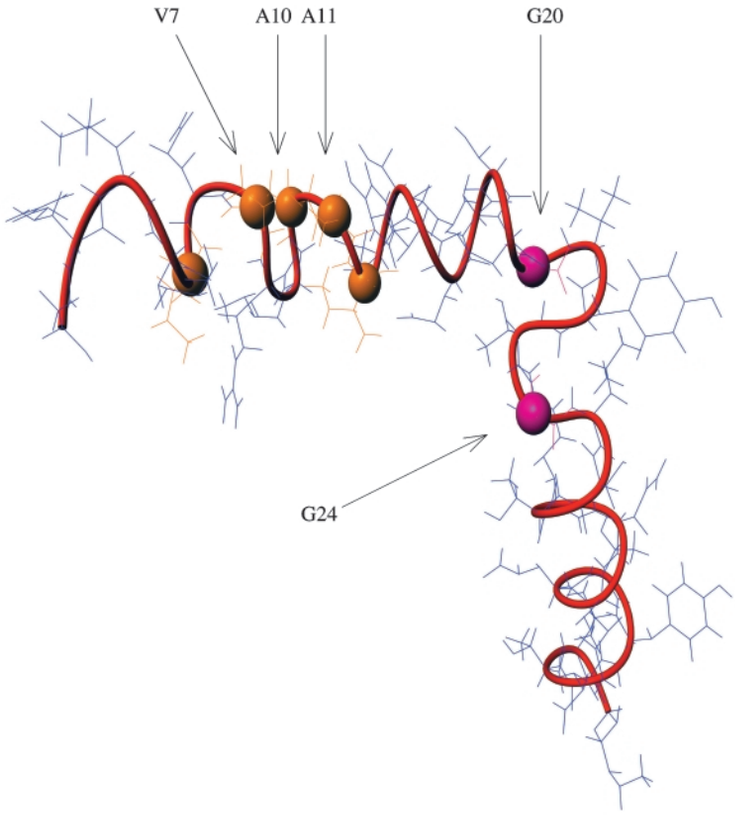

Fig. 4 The structure of the $Fc_{\varepsilon}R1$ γ-chain obtained from the constrained molecular dynamics simulations as described in the text, plotted using the program MOLMOL. This structure is a member of family **X**, and exhibits the fewest violations of the nOe constraints. The orange spheres show the positions of the α-carbons of the five hydrophobic residues in the N-terminal α-helix, and the pink spheres are the α-carbons of the glycine residues at either end of the β-bend.

annealing routine. For structures where this occurred, the simulation was restarted from the initial DIANA structure.

The 50 final structures were screened using the following criteria:[22] (a) the number of nOe constraint violations should be low (less than 10); (b) the relative energy of the structure obtained should be low; (c) the torsion angles obtained should fall within the known favoured ranges, checked by the use of Ramachandran plots[23] which were generated using the program PROCHECK.[24]

These structures may be grouped into 'families' and the structural integrity within a family is characterised by the minimised root mean square deviation (RMSD) between the positions of corresponding atoms in the individual structures. A family (called **X**) of nine structures satisfied the above criteria (a)–(c) and showed a pairwise RMSD less than 1.3 Å for the peptide backbone atoms of residues 5 to 35. The member of family **X** exhibiting the fewest nOe constraint violations is shown in Fig. 4. The conformation of the backbone is illustrated by a heavy line, and α-helical secondary structure can clearly be seen from residue 4 to 19 and from residue 25 to 36, with a disruption in the helix between residues 20 and 24.

An additional group of seven structures (family **Y**), from the same structure calculation also passed the screening criteria. These structures showed a close correlation (pairwise RMSD less than 1.3 Å) when fitted between residues 4 to 19, *or* between residues 25 to 35; both of these regions showing an α-helical structure similar to family **X**. The difference between the two families is the variable structure of the region comprising residues 20 to 24 for **Y**, because of variations in the backbone torsion angles. This region of variable structure therefore may be likened to a flexible 'hinge', and the structures of family **Y**, with the region of residues 4 to 19 overlaid, are shown in Fig. 5a, and with residues 25 to 35 overlaid in Fig. 5b. The variation of the torsion angles for residues 20 to 24 may be attributed to fewer nOe constraints defining this region of the chain. Within the region Gly-20 to Gly-24 there were 11 sequential inter-residue nOe constraints and just a single non-sequential inter-residue from Gly-20 α*H* to Thr-23 N*H*. There are 10 non-sequential inter-residue constraints involving just one residue from this region: Ser-18 to Val-21, Asp-19 to Tyr-22, Tyr-22 to Leu-25, and Gly-24 to Thr-27, and these also help to define this non-helical region. The lack of nOe constraints is partially due to overlap of peaks, however conformational averaging may cause the strong peaks expected for a well defined region to appear weak or absent. In this respect several important distance restraints, shown in Fig. 3, are longer than corresponding distances in the well defined helical regions. Certainly no reason can be found in the current data to discount the presence of the family **Y** structures, indeed the torsion angles do not show high steric hindrance in the Ramachandran plot. The ability to bend in this region of the structure may aid in the function of this peptide.

The nature of the disruption was then examined. The members of family **X** exhibit a hydrogen bond between Gly-20 and Thr-23, with an average distance between the C***O*** of the Gly-20 and the ***N***H of Thr-23 of 3.2 Å, and an average angle between the C***O***20, ***N***H23 and N***H***23 of 17°. Such a (i, $i + 3$) hydrogen bond is typical of a β-bend and therefore this region was examined for further evidence of this structure. Chou and Fasman[25] have classified a β-bend using the following criteria: (a) a hydrogen bond between the i and $i + 3$ residues must be present, and the C***O*** to ***N***H distance should be ≤3.5 Å; (b) the $C_{\alpha}i$ to $C_{\alpha}i + 3$ distance should be <7 Å; (c) bends that do not have torsion angles (φ, ψ)$i + 1$ and (φ, ψ)$i + 2$, differing by more than 50° from the "perfect" values are classified as ideal.

As discussed above, a hydrogen bond complying with condition (a) exits between residues 20 and 23; thus if a β-bend is present the first (ith) residue will be Gly-20. The average $C_{\alpha}20$ to $C_{\alpha}23$ distance of the family **X** structures is 4.8 Å, thus condition (b) is met. The $\varphi 21$ and $\psi 21$ of the final structures have average

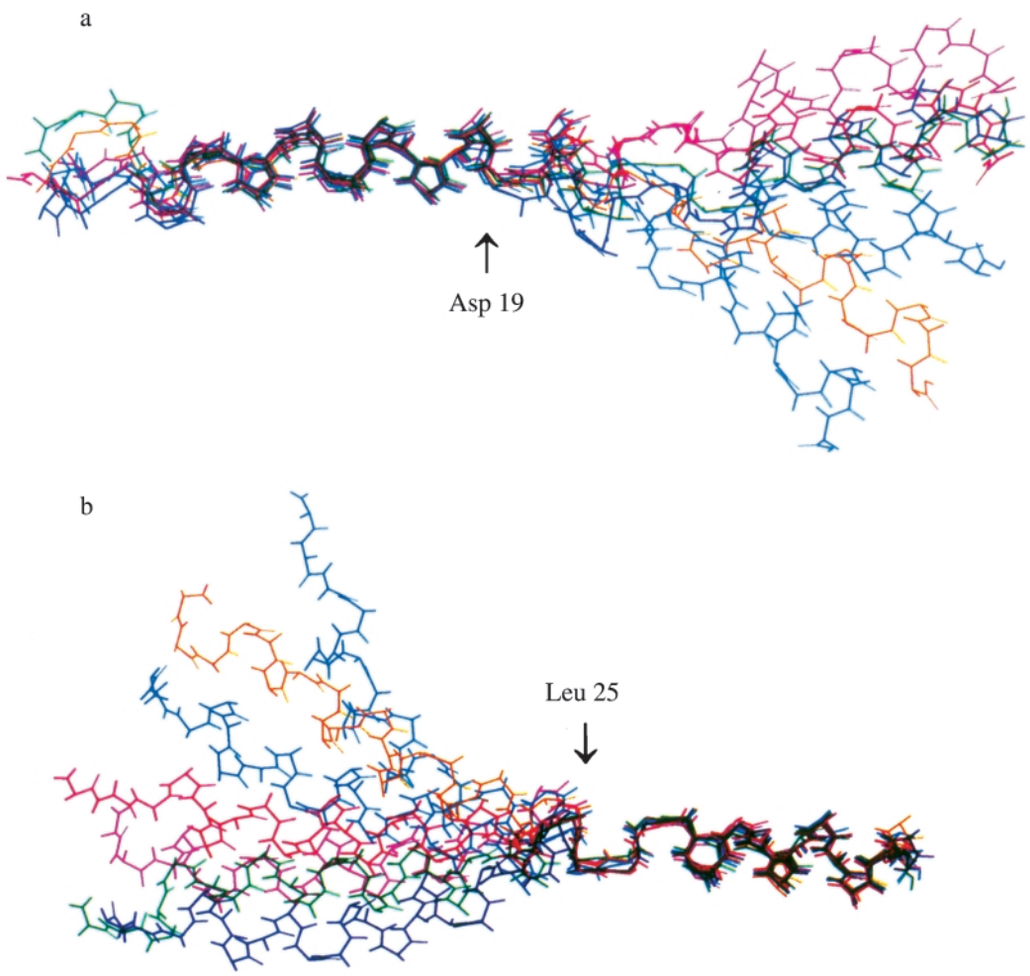

Fig. 5 The family **Y** structures of the $Fc_{\varepsilon}R1$ γ-chain obtained from the constrained molecular dynamics simulations as described in the text, plotted using the SYBYL software: (a) with residues 4 to 19 overlaid; (b) with residues 25 to 35 overlaid.

values of −65° and −14°, and the φ22 and ψ22 have average values of −137° and 39°. Venkatachalam[26] defined the perfect type I β-turn by φ and ψ (i + 1) torsion angles of −60° and −30° respectively, and φ and ψ (i + 2) torsion angles of −90° and 0°. Thus all the criteria given by Chou and Fasman[25] to define a type I β-turn are met.

Type I turns often involve a change in direction of the peptide backbone chain. This is not the case with the family **X** structures obtained here, and this is due to the backbone torsion angles of Gly-24, with averages for φ and ψ of −141° and 44° respectively, causing a straightening of the chain.

The use of TFE as solvent is widely known to promote secondary structure in peptides, although as discussed by Horne *et al.*[13] this secondary structure will only form where such a propensity already exists within the amino acid sequence.[27] Therefore the structures determined here may still be relevant to the *in vivo* activity of the $Fc_{\varepsilon}R1$ γ-chain. Although the solvent medium employed for detailed NMR analysis was 65% TFE-d_3, the secondary structural features were apparent at the much lower TFE-d_3 level of 26%, but the higher proportion of TFE-d_3 was used because of the somewhat improved spectral resolution it afforded (see Experimental section). That TFE-d_3 does not completely force the peptide into a helical conformation is illustrated by the disruption of the helix between residues Gly-20 and Gly-24, and also the exclusion of the N-terminal three residues and C-terminal two residues from the helix. It is important that glycine residues are generally considered[28] to be poor helix formers. The detailed study by Sonnichsen *et al.*[27] on the secondary structure of the actin 1–28 peptide in 80% TFE–water displayed two α-helical regions for residues 4–13 and for residues 16–20, separated by a β-turn, with the sequence of the turn region being Gly-13–Ser-14–Gly-15–Leu-16 (serine is also considered[28] to be a poor helix former). In addition even at this very high level of TFE used (80%) the 8 C-terminal residues did not show secondary structure. Horne *et al.*[13] used 28% TFE–water as solvent for the NMR structural study of the 36 residue neuropeptide K (NPK) and found well defined helical structure from residue Asp-3 to Gly-20, but found no evidence for a defined helix for the 16 C-terminal residues.

Modelling

Once the structure of the γ-chain had been determined, models were created to examine the important features of the structures and how these may participate in the function of the receptor *in vivo*.

Position of the hydrophobic residues. There are five hydrophobic residues in the N-terminal α-helix, and three of these (Val-7, Ala-10 and Ala-11) are grouped on one side of the helix as shown in Fig. 6a (see also Fig. 4). *In vivo* the γ-chain exists as a dimer, and the grouping of these hydrophobic residues indicates the possibility that the γ-chains associate *via* this feature.

Position of the conserved residues. The ARAM consensus motif,[5] based upon the YXXI/L sequence, comprises the residues Asp-19, Tyr-22, Leu-25, Tyr-33 and Ile-36 for the $Fc_{\varepsilon}R1$ γ-chain, and once this motif is phosphorylated, it is recognised by SH2 domains.[7] Two of these ARAM residues (Leu-25, Tyr-33) are in the C-terminal helix and two more (Tyr-22, Ile-36) are near. The positions of these residues in the lowest

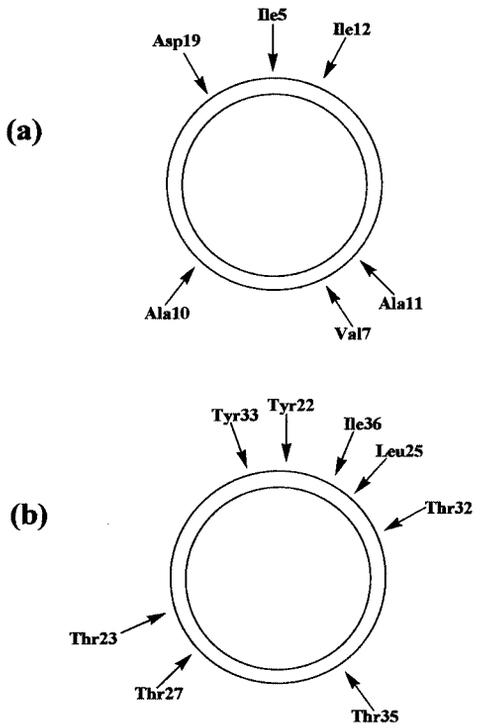

Fig. 6 Schematic representation of the α-helical regions of the family X structure shown in Fig. 4, the arrows indicate the relative positions of the α-carbons of the selected residues: (a) the N-terminal α-helix viewed along its axis in the direction Asp19→Leu3; (b) the C-terminal α-helix viewed along its axis in the direction Thr35→Leu25.

energy family **X** member are shown schematically in Fig. 6b, where the helix is viewed along its axis. The alignment of Leu-25 and Ile-36 forms a minor hydrophobic face. Waksman *et al.*[29] determined the X-ray structure of the complex between a high affinity 11-residue phosphopeptide and the Src SH2 domain. The peptide complexed in an extended conformation and the phosphotyrosine and isoleucine residues of the sequence pTyr–Glu–Glu–Ile bound to specific pockets on the SH2 domain. After tyrosine phosphorylation of the $Fc_{\varepsilon}R1$ γ-chain it is possible that there is a relaxation of the α-helical structure to accommodate the binding to SH2 domains. The role of the ARAM Asp-19, which is highly conserved, (shown in Fig. 6a) has not yet been determined. It is possible that it has an important role in receptor structure, aggregation or association with adjacent proteins, possibly by salt bridge formation, but in the crystallographic study by Waksman *et al.*[29] it was not shown to be necessary for binding of the SH2 domains.

Position of the threonine residues. The threonines of the γ-chain undergo phosphorylation rapidly after receptor aggregation.[30] Therefore the threonine residues might be exposed in order that they may interact with threonine kinases. In Fig. 6b the four threonine residues (23, 27, 32, 35) can be seen to be located on the same side of the C-terminal helix, away from the ARAM motif tyrosines.

Model of the γ-chain dimer. It is known that the γ-chain is a dimer in the receptor, and it has also been shown[31] that after antigen binding and aggregation the $Fc_{\varepsilon}R1$ receptor is phosphorylated at the threonine residues in addition to the tyrosines. Dimerisation may occur in a head-to-head fashion with the family **X** helices aligned more or less parallel, with the contact between the two hydrophobic faces of the two N-terminal helices. Tyr-22 and Tyr-33 and most of the threonine residues would be solvent exposed in such a dimer and therefore available for phosphorylation. The β-bend distortion after residue 21 would cause the two chains to diverge somewhat making Thr-23, -27, -32 and -35 more solvent exposed and therefore more readily available for phosphorylation. Dimerisation of two family **Y** helices may occur in a similar manner and could be thought to immobilise both helices in the region of residues 1 to 21, then the greater flexibility of the hinge regions would result in a possible 'scissoring' motion of the two C-terminal helical regions (residues 25 to 35, see Fig. 4b). Therefore the family **Y** dimers would also have Thr-23, -27, -32 and -35 solvent exposed.

Experimental

Sample preparation

A synthetic sample of the cytoplasmic portion of the γ chain of the human $Fc_{\varepsilon}R1$ receptor was provided in solid form by Glaxo Group Research Ltd. The purity and sequence of the compound were verified by sequencing of the first 21 residues, high pressure liquid chromatography (HPLC) and mass spectrometry. Samples of the peptide were prepared in water solution and in methanol–water (70 : 30 v/v), and ^{1}H NOESY NMR spectra measured (see below). However in these spectra there were no crosspeaks attributable to N*H*–N*H* contacts, and a minimum number of crosspeaks that could be assigned to other inter-residue contacts. The ^{1}H NOESY spectrum of another sample prepared in TFE-d_3–H_2O (26 : 74 v/v) did show the inter-residue crosspeaks characteristic of secondary structure, and increasing the proportion of TFE-d_3 to 40% and to 65% by volume had the additional beneficial effect of improving somewhat the resolution of the ^{1}H spectrum.

The NMR samples for detailed analysis were prepared with 3.5 mg of the solid peptide dissolved in 0.7 ml of TFE-d_3–water (65 : 35 v/v) and TFE-d_3–D_2O (65 : 35 v/v). The pH of both samples was 3.3 as measured using a model 7020 pH meter (Electronic Instruments Ltd). These solutions were then transferred to 5 mm od Wilmad 528-PP-7 NMR tubes.

NMR data

All ^{1}H NMR data were collected on Bruker AMX600 spectrometers (14.2 T). The 2-dimensional spectra were recorded in phase-sensitive mode using either time-proportional phase incrementation (TPPI)[32] or States-TPPI[33] quadrature detection.

For the TFE-d_3–water sample the spectra were measured at 290 and 300 K. The NOESY 2D spectra were measured with mixing times 50, 100 and 200 ms, using low power irradiation to suppress the water signal during a 2 s relaxation delay between the acquisition of transients and during the mixing time. The TOCSY 2D spectrum used the DIPSI-2[34] spin lock for 100 ms, and again solvent suppression during a 2 s relaxation delay. A double quantum filtered (DQF) COSY spectrum was also measured with solvent suppression during the 2 s relaxation delay. Typical acquisition parameters were with spectral widths approximately 7 kHz, with 2048 data points acquired in t_2, and 512 increments in t_1. 64 transients were acquired for each increment giving an experiment time *ca.* 16 h. For the measurement of the $^3J_{\alpha N}$ couplings a DQF-COSY spectrum with greater digital resolution was acquired, employing 8192 acquisition data points in t_2 and 1024 increments in t_1.

For the TFE-d_3–D_2O sample the NOESY, TOCSY and DQF-COSY spectra were measured at 290 K as described above.

All 2D NMR data sets were processed using NMRz/Tripos software on a Silicon Graphics workstation. The FIDs of the spectra were apodized using a 90° shifted sine-bell function in both t_1 and t_2 dimensions, and the t_1 dimension was zero-filled prior to Fourier transformation. Base-plane flattening was performed using a series of linear corrections to the data in both dimensions. The highly digitised COSY spectrum was processed using a 60° shifted sine-bell function. The vicinal coupling constants were measured by selecting individual rows

of transformed data containing the antiphase peaks of interest, inverse Fourier transformed, zero filled to 32768 data points, and transformed again. The resulting effective digital resolution was 0.85 Hz point^{-1}.

Molecular dynamics simulations

Simulated annealing was performed using the SYBYL molecular modelling package produced by Tripos Inc. SYBYL uses the following terms within the Tripos force field[35] to apply distance constraints as a range: $E_{range} = 0$, when $d_{low} \leq d \leq d_{high}$; $E_{range} = \frac{1}{2}\ k_{range}(d - d_{low})^2$, when $d < d_{low}$; $E_{range} = \frac{1}{2}\ k_{range}(d_{high} - d)^2$, when $d_{high} < d$. Where d is the interproton distance; d_{low} is the lower bound of the range; d_{high} is the upper bound of the range; k_{range} is the force constant in kcal mol^{-1} Å^{-2} and E_{range} is the potential energy penalty for exceeding the prescribed constraint bounds.

The torsion angle constraints were removed and the distance range constraint force constant k_{range} was reduced to 2 kcal mol^{-1} Å^{-2} for all the DIANA generated structures. Each of the 50 structures was heated to 1750 K. Initial velocities were assigned randomly and a step size of 0.2 fs was employed during all simulations. The structures were cooled to 1000 K over 5000 fs; during this period the k_{range} was gradually increased to 15 kcal mol^{-1} Å^{-2}. The annealing process was continued by further cooling of the structures to 300 K over a period of 3000 fs, whilst the k_{range} was kept constant at 15 kcal mol^{-1} Å^{-2}. At the end of this procedure the dynamic simulations were allowed to continue at 300 K for 500 fs. A dynamic "history" was then compiled for each structure during the 300 K period of the simulation. (A dynamic history consists of a set of conformations sampled by a structure at user-defined time intervals during a molecular dynamics run; 20 fs intervals were used here.) The conformation showing the lowest potential energy was selected from the history file of each structure; these were then subjected to 2000 steps of conjugate gradient energy minimisation to give the final structures.

Both SYBYL and the program MOLMOL[36] were used to plot the structures.

Acknowledgements

One of us (M. K. E.) wishes to thank the EPSRC and Glaxo Group Research for the award of a CASE studentship. We thank Glaxo for use of a 600 MHz NMR spectrometer, and the University of London Intercollegiate Research Service (ULIRS) at QMW for 600 MHz NMR spectra and for use of the Silicon Graphics workstation with the Tripos SYBYL software package. Structures were plotted using either the SYBYL software or the MOLMOL package, with the assistance of Mr A. Beanie, Department of Biochemistry at QMW and Dr H. Toms, Department of Chemistry at QMW. We acknowledge many revealing and useful discussions with Dr Brian Sutton of the Randall Institute, King's College, London, on the modelling results.

References

1 H. J. Gould and B. J. Sutton, *Nature*, 1993, **366**, 421.
2 C. Ra, M.-H. E. Jouvain, U. Blank and J.-P. Kinet, *Nature*, 1989, **341**, 752.
3 H. Kuster, H. Thomson and J.-P. Kinet, *J. Biol. Chem.*, 1990, **265**, 6448.
4 S. Amigorena, J. Salamero, J. Davoust, W. H. Fridman and C. Bonnerot, *Nature*, 1992, **358**, 337.
5 M. Reth, *Nature*, 1992, **338**, 383.
6 A. D. Keegan and W. E. Paul, *Immunol. Today*, 1992, **13**, 63.
7 J. A. Cooper, *Semin. Cell. Biol.*, 1994, **5**, 377.
8 I. L. Barsukov and L. Y. Lian, in *NMR of Macromolecules*, ed. G. C. K. Roberts, IRL Press, Oxford, 1993, pp. 315–357.
9 D. S. Wishart, B. D. Sykes and R. M. Richards, *J. Mol. Biol.*, 1990, **222**, 311.
10 V. J. Baus, *Methods Enzymol.*, 1989, **177**, 132.
11 D. Neuhaus, G. Wagner, M. Vasak, J. H. R. Kägi and K. Wüthrich, *Eur. J. Biochem.*, 1985, **151**, 257.
12 M. Billeter, W. Braun and K. Wüthrich, *J. Mol. Biol.*, 1982, **155**, 321.
13 J. Horne, M. Sadek and D. J. Craik, *Biochemistry*, 1993, **32**, 7406.
14 W. F. Walkenhorst, A. M. Krezel, G. I. Rhyu and J. L. Markley, *J. Mol. Biol.*, 1994, **242**, 215.
15 K. Wüthrich, M. Billeter and W. Braun, *J. Mol. Biol.*, 1983, **169**, 949.
16 P. Güntert, W. Braun and K. Wüthrich, *J. Mol. Biol.*, 1991, **217**, 517.
17 W. P. Purcell and J. A. Singer, *J. Chem. Eng. Data*, 1967, **12**, 235.
18 J. Gasteiger and M. Marsili, *Tetrahedron*, 1980, **36**, 3219.
19 D. F. Mierke and H. Kessler, *Biopolymers*, 1993, **33**, 1003.
20 *Lange's Handbook of Chemistry*, 12th edn., ed. J. A. Dean, McGraw Hill, New York, 1979, pp. 10–99.
21 S. Kirkpatrick, C. D. Gelatt and M. P. Vecchi, *Science*, 1983, **220**, 671.
22 M. J. Sutcliffe, in *NMR of Macromolecules*, ed. G. C. K. Roberts, IRL Press, Oxford, 1993, pp. 359–390.
23 G. N. Ramachandran and V. Sasisekharan, *Adv. Protein Chem.*, 1968, **23**, 283.
24 A. L. Morris, M. W. MacArthur, E. G. Hutchinson and J. M. Thornton, *Proteins: Struct., Funct., Genet.*, 1992, **12**, 345.
25 P. Y. Chou and G. D. Fasman, *J. Mol. Biol.*, 1977, **115**, 135.
26 C. M. Venkatachalam, *Biopolymers*, 1968, **6**, 1425.
27 F. D. Sonnichsen, J. E. Van Eyk, R. S. Hodges and B. D. Sykes, *Biochemistry*, 1992, **31**, 8790.
28 See for example J. S. Richardson, *Adv. Protein Chem.*, 1981, **34**, 167.
29 G. Waksman, S. E. Shoelson, N. Pant, D. Cowburn and J. Kuriyan, *Cell*, 1993, **72**, 779.
30 R. Paolini, M.-H. Jouvin and J.-P. Kinet, *Nature*, 1991, **353**, 855.
31 W. Li, G. G. Deanin, B. Margolis, J. Schlessinger and J. M. Oliver, *Mol. Cell. Biol.*, 1992, **12**, 3176.
32 G. Drobny, A. Pines, S. Sinton, D. Weitekamp and D. Wemmer, *Faraday Symp. Chem. Soc.*, 1978, **13**, 49.
33 D. J. States, R. A. Haberkorn and D. J. Ruben, *J. Magn. Reson.*, 1982, **48**, 286.
34 A. J. Shaka, C. J. Lee and A. Pines, *J. Magn. Reson.*, 1988, **77**, 274.
35 M. Clark, R. D. Cramer and N. Van Opdenbosch, *J. Comput. Chem.*, 1989, **10**, 982.
36 R. Koradi, M. Billeter and K. Wüthrich, *J. Mol. Graphics*, 1996, **14**, 51.